17

Method of selection of objects on a hyperspectral image based on the analysys of their contours

© V.V. Shipko, M.F. Volobuev

Air Force Military Training and Research Centre Air Force Academy
named after professor N.E. Zhukovskiy and Yu.A. Gagarin,
394064 Voronezh, Russia

e-mail: shipko.v@bk.ru

Received February 17, 2022
Revised March 22, 2022
Accepted April 10, 2022

A new method of spectral selection of given objects on hyperspectral images is considered. At the first stage of the method, hypotheses are tested using the Neyman–Pearson criterion about the presence of object contours in neighboring pixels relative to the simple alternative of their absence consistently over all spectral components. If a decision is made about the presence of a contour in at least one spectral channel, these pixels are analyzed at the second stage with respect to their distribution over the spectral range according to the criterion of maximum a posteriori probability density. Given the values of the mathematical expectation of the gradient difference between the spectral components, hypotheses are formed about the presence or absence of the contour of the desired object. The decision is made on the basis of a comparison of the decision statistics with the likelihood functions. The characteristics of detection and the results of experiments performed on real images are presented.

Keywords: hyperspectral images, contour, gradient, likelihood function.

DOI: 10.21883/EOS.2022.08.54774.3268-22

Introduction

Today, an intensive development and implementation of the hyperspectral imaging technologies are observed in various fields of human?s activities. Modern prototypes of hyperspectral hardware allow to take images in hundreds of narrow stripes of ultraviolet, visible and near infrared ranges of the spectrum [1,2]. One of the critical problems of processing of hyperspectral images (HSI) is detection (selection) of objects on various backgrounds. More frequently, this problem is solved by selecting the object contours [3]. The contour refers to gradient difference (a jump-like discontinuity) in brightness that exceeds a certain value. The use of contour images allows to significantly reduce computational costs of different algorithms of further analysis and recognition, which is especially actual for processing of multicomponent HSI.

There are many methods and algorithms of selecting contours on single-component images [3–9]. Some of them are based on the use of gradient operators [3], others use statistical [4–6] or neural network [5,6] approach; there are also algorithms based on the methods of mathematical morphology [7], rank algorithms, [8] etc. [9]. However, the most of the existing methods and algorithms of selecting the contours on single-component images has poor efficiency in case of component-by-component processing of multicomponent HSI. It is generally related with the absence of possibility to consider interrelations between spectral components. Serial analysis of a contour of each spectral channel is a challenging and ineffective problem, and averaging the obtained results leads to the loss of valuable information on the spectral interrelation. There are, for example, specific problems, which are typical only for HSI processing [10,11], where it is required to select the objects with spectral characteristics similar to those from the spectral library or to select the objects within certain spectral range etc. Here, all existing algorithms [3–9] of contours selection can be used only at the preliminary stage of the HSI contours analysis. The papers [12,13] justified the approaches and reviewed some algorithms of contour selection on HSI, allowing to take into account interspectral correlation, however, the contours detection threshold and the problem formulation itself are of euristic nature.

The goal hereof is to develop a method for the selection of objects on hyperspectral image based on the statistical analysis of their contours.

Problem formulation

The model of a L-component hyperspectral image $\mathbf{\Lambda}$ digitalized by i lines and j columns in general case has the following view

$$\mathbf{\Lambda} = [\lambda^1_{i,j}, \lambda^2_{i,j}, \ldots, \lambda^L_{i,j}],\ \lambda^l_{i,j} \in [0, \ldots, 2^N - 1], \qquad (1)$$

where $i = 1, \ldots, I,\ j = 1, \ldots, J$; I, J — number of lines and columns of the image, accordingly; l — HSI component index, $l = 1, \ldots, L$; N — degree of quantization of the image components brightness $\mathbf{\Lambda}$.

Subject to effect from various factors during the formation of separate spectral components of HSI, the model of such

Combination of joint pairs of values of indices i, j and p, q

$n_{i,j}$	1	2	3	4
p	i	$i+1$	$i+1$	$i-1$
q	$j+1$	j	$j+1$	$j+1$
i, j	$1, \ldots, I,$ $1, \ldots, J-1$	$1, \ldots, I-1,$ $1, \ldots, J$	$1, \ldots, I-1,$ $1, \ldots, J-1$	$2, \ldots, I,$ $1, \ldots, J-1$

image can be represented as an adaptive mixture of useful component $\mathbf{\Lambda}$ and noise:

$$\mathbf{X} = \mathbf{\Lambda} + \boldsymbol{\eta} = [x^1_{i,j}, x^2_{i,j}, \ldots, x^L_{i,j}],\ x^l_{i,j} \in [0, \ldots, 2^N - 1], \tag{2}$$

where $\boldsymbol{\eta} = [\eta^1, \eta^2, \ldots, \eta^L]$ — is accidental spectral and spatially not correlated additive noise component of signals of an L-component image with zero mathematical expectation (ME) and some value of the root mean square error (RMSE) σ^l_x. Adequacy of such noise model for many applications is quite justified in a series of papers, for example, in [5,10,14]. Then, we are to consider that the brightnesses $x^l_{i,j}$ of each pixel of HSI $\mathbf{X}$ are independent, not displaced, distributed according to normal law with unknown mathematical expectation $m^l_{x_{i,j}}$ and known RMSE σ^l_x:

$$W(x^l_{i,j}) = \frac{1}{\sqrt{2\pi}\sigma_x} \exp\left(-\frac{(x^l_{i,j} - m^l_{x_{i,j}})^2}{2(\sigma^l_x)^2}\right). \tag{3}$$

An indication of the absence of the object contour on HSI is the coincidence of ME of scalar values of brightness of neighboring pixels with some permissible deviation $m^l_{x_{i,j}} \approx m^l_{x_{i\pm1,j\pm1}} = m^l$. An indication of presence of the object to be found is the coincidence of the probabilistic characteristics of its contour with those defined a priori.

We will consider pair-by-pair comparison of the values of brightness of i, j-th pixels and neighboring p, q-th pixels with an unknown true value m^l.

Table represents n pair combinations of i, j-th and neighboring p, q-th pixels corresponding to them, used in their joint evaluation.

According to the conditions given above, the process of selection of the contour of the object to be found will be in two steps.

The first step — finding the object contours on HSI.

The second step — contour selection with the required probabilistic parameters.

Description of the method

At the first stage we use the Neyman–Pearson criterion for the hypotheses testing [15,16] in the following variant:

— let us test the H_0 hypothesis on the absence of image contours in neighboring pixels versus a simple alternative of their presence H_1, wherein the test is performed in series by all spectral components l;

— in case of deciding on the presence of the contour in at least one spectral component, these pixels are analyzed at the second stage.

At the second stage we use the criterion of maximum a posteriori probability density [15,16]. Then making a decision as to the presence of a contour with the required parameter generally reduced to checking the hypothesis versus a simple alternative: no contour with the required parameter. For this we form a likelihood function versus the required ME and the likelihood function for any low deviation of ME whatsoever from its required value. Then, by using the likelihood ratio and the specified criterion we assume one or another hypothesis. However, for small selections an accurate knowledge of the ME within the whole spectral range is complicated, usually, we know the permissible range of ME deviation of the contour to be found. So, we can use the hypothesis test versus a complex alternative as follows. Having stated the values of mathematical expectation of the difference of gradients in spectral components, let us form hypotheses: H_2 — presence of the contour with the specified parameter; H_3 — there is no contour with the specified parameter, the brightness discontinuity is too high; H_4 — there is no contour with the specified parameter, the brightness discontinuity is too low.

Stage 1. In accordance with the selected procedure of the hypotheses testing, we identify the hypotheses likelihood functions and assess their unknown parameters.

For the accepted models the likelihood function as the probability density of the measured parameter values with its known true value is described by the multidimensional normal law of distribution.

In case of zero hypothesis about the absence of the object contours on HSI, its likelihood function depends on one unknown informational parameter m^l:

$$W^l_n(m^l) = \frac{1}{2\pi\sigma^2_x} \exp\left(-\frac{(x^l_{i,j} - m^l)^2 + (x^l_{p,q} - m^l)^2}{2(\sigma^l_x)^2}\right), \tag{4}$$

where p, q — parameters of pixels of the vicinity, determined in accordance with Table; n — the number of analyzed pair of pixels with the coordinates i, j and p, q.

In order to find an optimum value of the unknown parameter we use the method of maximum likelihood. For this, let us take logarithm of the likelihood function (4) and differentiate it:

$$\ln\left(W^l_n(m^l)\right) = \ln\left(\frac{1}{2\pi\sigma^2_x}\right) - \frac{(x^l_{i,j} - m^l)^2 + (x^l_{p,q} - m^l)^2}{2(\sigma^l_x)^2}, \tag{5}$$

$$\frac{\partial \ln\left(W^l_n(m^l)\right)}{\partial m^l} = \frac{(x^l_{i,j} - m^l)^2 + (x^l_{p,q} - m^l)^2}{(\sigma^l_x)^2}. \tag{6}$$

Having equalized the obtained value to zero, we obtain the optimum value of mathematical expectation

$$\hat{m}^l = \frac{x^l_{i,j} + x^l_{p,q}}{2}. \tag{7}$$

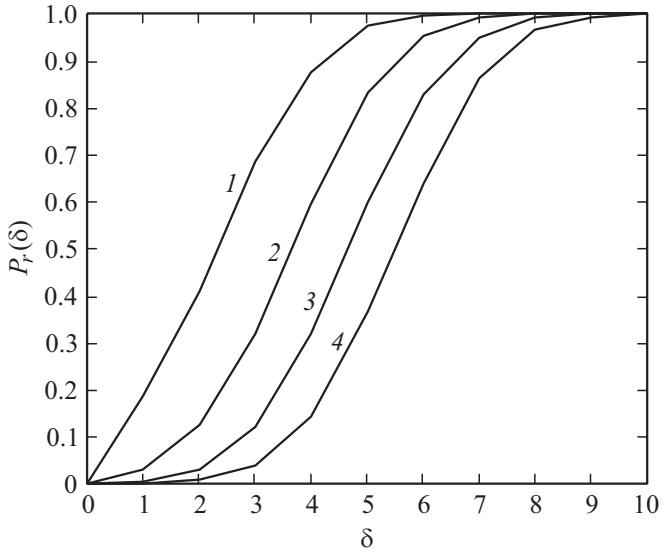

Figure 1. The probability of correct detection of the object contour at: *1* — $P_{f0} = 0.1$, *2* — $P_{f0} = 10^{-2}$, *3* — $P_{f0} = 10^{-3}$, *4* — $P_{f0} = 10^{-4}$.

The determinant statistics is as follows:

$$r^l_{n_{i,j}} = \frac{\left((x^l_{i,j} - \hat{m}^l)^2 + (x^l_{p,q} - \hat{m}^l)^2\right)}{(\sigma^l_x)^2}. \qquad (8)$$

The paper [17] shows that such a determinant statistics has the chi-square distribution with one degree of freedom. Then the threshold will be calculated based on the specified probability of false alarm P_{f0} by reverse functions of distribution

$$h_0 = \chi^{-2}(1 - P_{f0}; 1). \qquad (9)$$

The decision of the presence of object contours on HSI is taken by comparing the determinant statistics (8) with the threshold h_0,

$$r^l_{n_{i,j}} \underset{H_0}{\overset{H_1}{\geq}} h_0. \qquad (10)$$

In case of no excess of the threshold h_0 the hypothesis H_0 is adopted on the absence of the object contours in the analyzed pixels within this spectrum, otherwise, we assume the hypothesis H_1 on the presence of the contour in pixels of the n-the pair. In case if at least for one of the n pairs for the i, j-th pixel in the l-th spectral component the hypothesis H_1, is adopted, then this pixel is assigned 1, in other cases — 0:

$$r^l_{i,j} = \begin{cases} 1, & \forall n,\ \exists r^l_{n_{i,j}} \geq h_0, \\ 0, & \text{other cases.} \end{cases} \qquad (11)$$

The general decision on the presence of the contour in the i, j-th pixel for all spectral components of HSI is taken in case if $\forall l$, $\exists r^l_{i,j} = 1$.

Fig. 1 shows probabilities of correct detection of the P_r contour of object depending on the deviation

$$\delta = \frac{|m^l_{i,j} - m^l_{p,q}|}{(\sigma^l_x)^2},$$

obtained as a result of statistical modelling with the selection volume in each point of the analysis 10 000.

Stage 2. In case when the decision is made on the presence of the contour in the i, j-th pixel, we will perform its further analysis relative its distribution by the spectral range.

We will use the brightness gradients $g_{i,j}$, obtained by any operators (Roberts, Sobel, Prewitt, Laplace, etc. [3]) as the values to be analyzed. The vector of scalar values of HSI brightness gradients subject to spectrum, where the image is analyzed, has the following view:

$$\mathbf{G} = \mathrm{Grad}[\mathbf{X}] = [g^l_{i,j}, g^2_{i,j}, \ldots, g^L_{i,j}], \qquad (12)$$

where Grad[. . .] — gradient operator.

Since the image gradients are obtained by using the difference equations with constant coefficients, the normal brightness change law (3) turns to the normal gradients change law:

$$W(g^l_{i,j}) = \frac{1}{\sqrt{2\pi}\sigma_g} \exp\left(-\frac{(g^l_{i,j} - m^l_{g_{i,j}})^2}{2(\sigma^l_g)^2}\right), \qquad (13)$$

where

$$\sigma_g = \frac{a\sigma_x}{b},\ m^l_{g_{i,j}} = n^{-1}\left(nm^l_{i,j} - \sum_{p=0}^{1}\sum_{q=0}^{1} m^l_{i\pm p, j\pm q}\right),$$

a is determined by weight coefficients of gradient filters (masks), b — number of the used paired elements of the mask for the gradient calculation.

The brightness gradients difference probability density in two spectral components will be [18]

$$W(\varphi^{1-2}) = \left(\frac{1}{2\sqrt{\pi}\sigma_g}\right) \exp\left(\frac{(\varphi^{1-2} - m_{\varphi^{1-2}})^2}{4(\sigma^l_g)^2}\right), \qquad (14)$$

where $\varphi^{1-2} = (g^1_{i,j} - g^2_{i,j})$, $m_{\varphi^{1-2}} = (m^1_{g_{i,j}} - m^2_{g_{i,j}})$.

Then, the total difference probability density of all possible pairs of gradients of each l-th component with the gradients of the rest of r-th components (without repetitions) is represented as

$$W_x(\varphi^{l-(l+r)}) = \left(\frac{1}{2\sqrt{\pi C_L}\sigma^l_g}\right) \times \exp\left(\frac{\left(\sum\limits_{r=1}^{L-1}\sum\limits_{l=1}^{L-r} \varphi^{l-(l+r)} - m_{\varphi^{l-(l+r)}}\right)^2}{4C_L(\sigma^l_g)^2}\right), \qquad (15)$$

where

$$\varphi^{l-(l+r)} = (g^l_{i,j} - g^{l+r}_{i,j}), \quad m_{\varphi^{l-(l+r)}} = (m^l_{g_{i,j}} - m^{l+r}_{g_{i,j}}),$$

$$C_L = \frac{L!}{(L-2)!2!}$$

— number of all possible paired combinations (without repetitions) of the differences of gradients composed of L spectral components, $r = 1, \ldots, L-1$.

In case, when it does not matter during the analysis of contour, in which certain pixel the ME is higher, it is expedient to use the sum of difference modul of the interspectral brightness gradients

$$\Delta = \sum_{r=1}^{L-1} \sum_{l=1}^{L-r} |g_{i,j}^{l} - g_{i,j}^{l+r}|.$$

At that the component

$$\Delta^r = \frac{1}{L-r} \sum_{l=1}^{L-r} |g_{i,j}^{l} - g_{i,j}^{l+r}|$$

in fact is the structural function of spectral gradients, and $\frac{\Delta}{C_L}$ — its ME. In order to simplify the expression, by introducing the new designation

$$\Theta_\Delta = \sum_{r=1}^{L-1} \sum_{l=1}^{L-r} m_{g_{i,j}}^{l} - m_{g_{i,j}}^{l+r}$$

based on the approaches stated in [18,19], we obtain

$$W(\Delta) = \left(\frac{1}{2\sqrt{\pi C_L}\sigma_g^l}\right)^k \sum_{k=0}^{K} C_K^k \exp\left(-\frac{(\Delta_k + \Theta_\Delta)^2}{4C_L(\sigma_g^l)^2}\right)^{K-k} \times \exp\left(-\frac{(\Delta_k - \Theta_\Delta)^2}{4C_L(\sigma_g^l)^2}\right)^k, \tag{16}$$

where C_K^k — binominal coefficient, $k = 1, \ldots, K$ — quantity of measurements.

Such expression is considerably simplified, if the deviation modulus of ME of the brightness gradients between spectral components is enough information during the contour analysis. In this case due to a low value of the exponent

$$\exp\left(-\frac{(\Delta_k + \Theta_\Delta)^2}{4C_L(\sigma_g^l)^2}\right)$$

it can be ignored, therefore

$$W(\Delta) = \left(\frac{1}{2\sqrt{\pi C_L}\sigma_g^l}\right)^k \exp\left(-\frac{\sum\limits_k (\Delta_k - \Theta_\Delta)^2}{4C_L(\sigma_g^l)^2}\right). \tag{17}$$

In this case logarithms of the likelihood functions of a complex alternative with exclusion of iterating multipliers

$$\left(\frac{1}{2\sqrt{\pi C_L}\sigma_g^l}\right)$$

are

$$W_\Delta(\Theta_2) = \left(-\frac{\sum\limits_k (\Delta_k - \Theta_2)^2}{4C_L(\sigma_g^l)^2}\right), \tag{18}$$

$$W_\Delta(\Theta_3) = \left(-\frac{\sum\limits_k (\Delta_k - \Theta_3)^2}{4C_L(\sigma_g^l)^2}\right), \tag{19}$$

$$W_\Delta(\Theta_4) = \left(-\frac{\sum\limits_k (\Delta_k - \Theta_4)^2}{4C_L(\sigma_g^l)^2}\right), \tag{20}$$

where the lower index — number of a hypothesis in the complex hypothesis, $\Theta_{2,3,4}$ — values of mathematical expectations specified a priori and corresponding to the hypotheses described above.

The determinant statistics is as follows:

$$r = \max\big(W_\Delta(\Theta_2),\ W_\Delta(\Theta_3),\ W_\Delta(\Theta_4)\big). \tag{21}$$

Making a decision as to the presence or absence of the object to be found on HSI is performed based on the comparison of the determinant statistics (21) with the likelihood functions (18)–(20),

$$r \overset{H_2}{=} W_\Delta(\Theta_2),\ r \overset{H_3}{=} W_\Delta(\Theta_3),\ r \overset{H_4}{=} W_\Delta(\Theta_4). \tag{22}$$

Therefore, contour images of the objects to be found in accordance with the first and the second stages are determined by the expression

$$c_{i,j} - \begin{cases} 0, & \text{if } H_0, \\ 1, & \text{if } H_1 \text{ and } H_2, \\ 2, & \text{if } H_1 \text{ and } H_3, \\ 3, & \text{if } H_1 \text{ and } H_4. \end{cases} \tag{23}$$

Examples of images processing

Fig. 2 shows selective HSI obtained by acoustic and optical hyperspectrometer [2] within a wide spectral range (500–750 nm) with the interval of 50 nm. Fig. 3 shows selective HSI obtained within a narrow spectral range (745–770 nm) with the interval of 5 nm. The images include two spectrally selective objects (object 1 — lower cube, object 2 — upper cube) having spectral characteristics, which are similar in terms of change, but different in terms of intensity, as shown in Fig. 4, where curve *1* — object 1, *2* — object 2, *3* — shadow, *4* — background.

In accordance with the first stage of the developed method, Fig. 5 presents the results of detection of contours by selections of images in Fig. 3, 4 by the optimum algorithm according to the Neyman–Pearson criterion (4)–(11) at different specified values of the false alarm probability values.

It should be noted that in case of non-conformance of the obtained distributions of pixels brightness with the normal law the first stage efficiency is sharply decreased. In this case increasing the efficiency is possible only by using other algorithms at the first stage, including that based on neural networks [5,6]. But, as shown by the results of processing of real HSI, the developed algorithm allows to obtain acceptable results for repeating the second processing stage.

In accordance with the second stage we calculated gradients of HSI components by means of the Prewitt

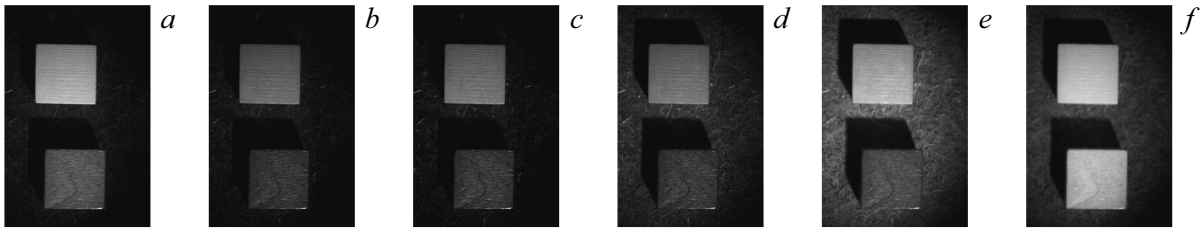

Figure 2. Selection of HSI components within wide spectral range: *a* — 500 nm, *b* — 550 nm, *c* — 600 nm, *d* — 650 nm, *e* — 700 nm, *f* — 750 nm.

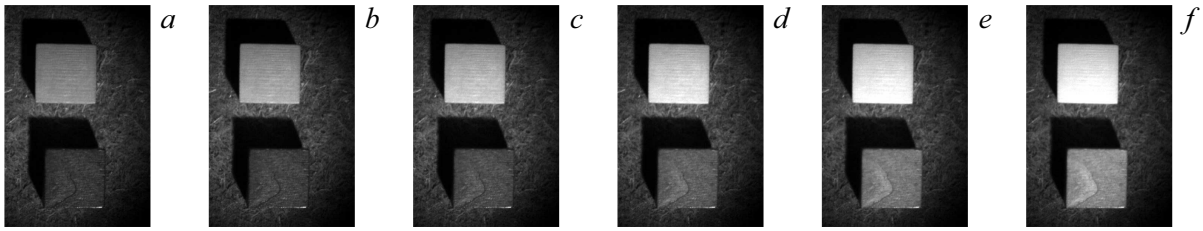

Figure 3. Selection of HSI components within narrow spectral range: *a* — 745 nm, *b* — 750 nm, *c* — 755 nm, *d* — 760 nm, *e* — 765 nm, *f* — 770 nm.

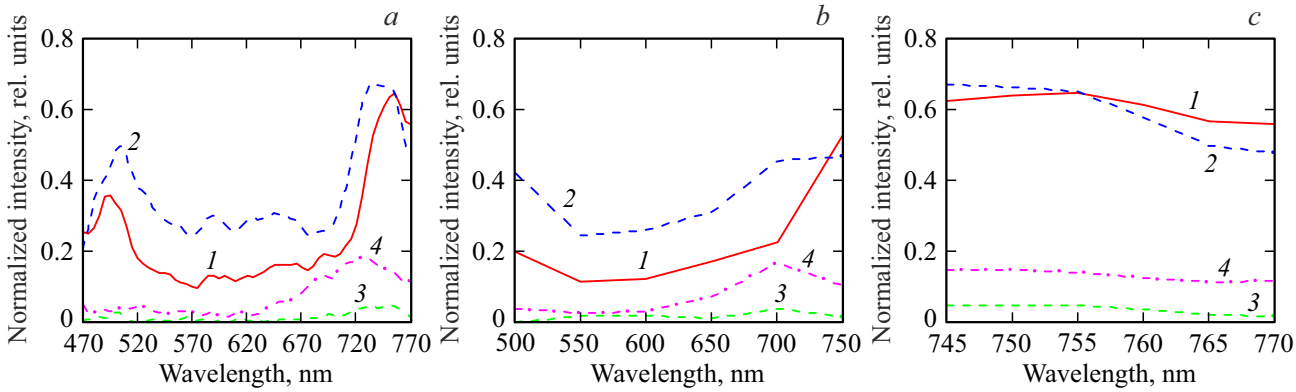

Figure 4. Normalized spectral intensities of reflection: (*a*) of the full set (61 spectral components within the range 470–770 nm with the interval 5 nm), (*b*) of six spectral components within a wide range 550–750 nm with the interval of 50 nm, (*c*) of six spectral components within a narrow range 745–770 nm with the interval 5 nm.

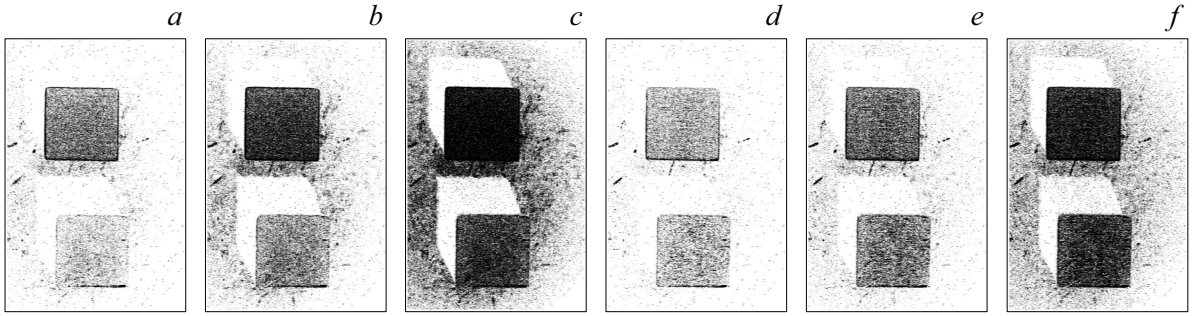

Figure 5. The result of detection of contours at the first stage: for the set of HSI (Fig. 2) at $P_{f0} = 10^{-4}$ — *a*, 10^{-3} — *b*, 10^{-2} — *c*, for the set of HSI (Fig. 3) at $P_{f0} = 10^{-4}$ — *d*, 10^{-3} — *e*, 10^{-2} — *f*.

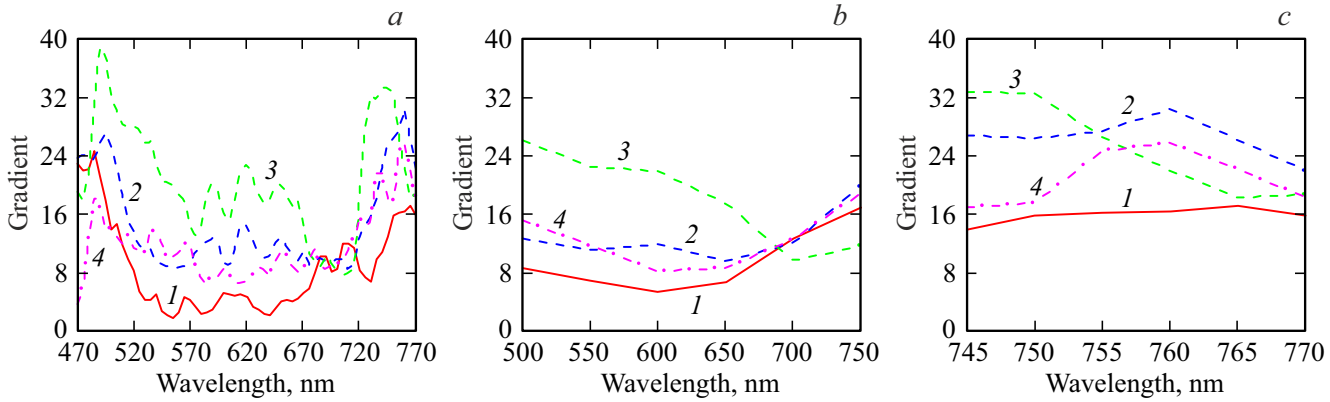

Figure 6. The values of HSI gradients: (*a*) of the full set (61 spectral component within the range 470–770 nm with the interval 5 nm), (*b*) of six spectral components within a wide range 550–750 nm with the interval of 50 nm, (*c*) of six spectral components within a narrow range 745–770 nm with the interval 5 nm.

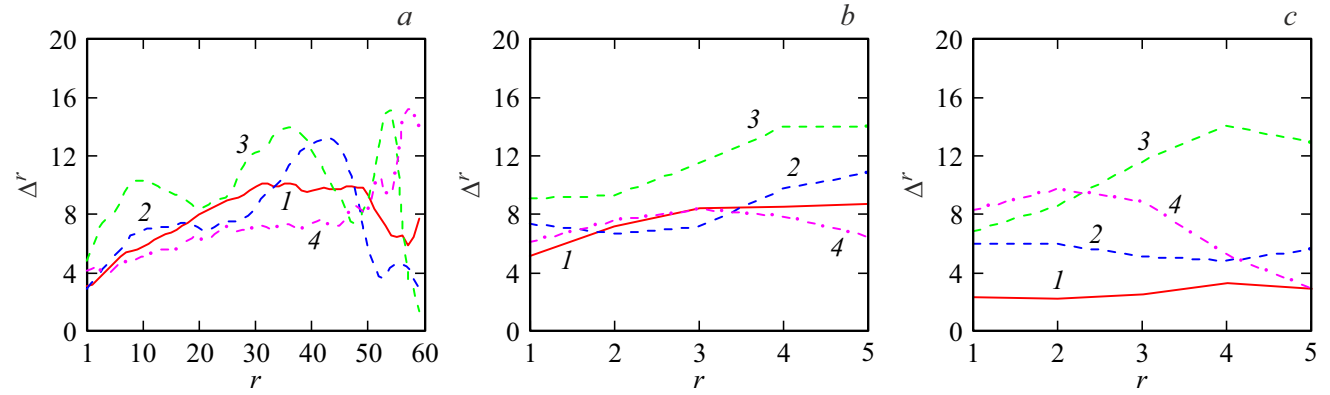

Figure 7. Structural functions of spectral components: (*a*) of the full set (61 spectral component within the range 470–770 nm with the interval 5 nm), (*b*) of six spectral components within a wide range 550–750 nm with the interval of 50 nm, (*c*) of six spectral components within a narrow range 745–770 nm with the interval 5 nm.

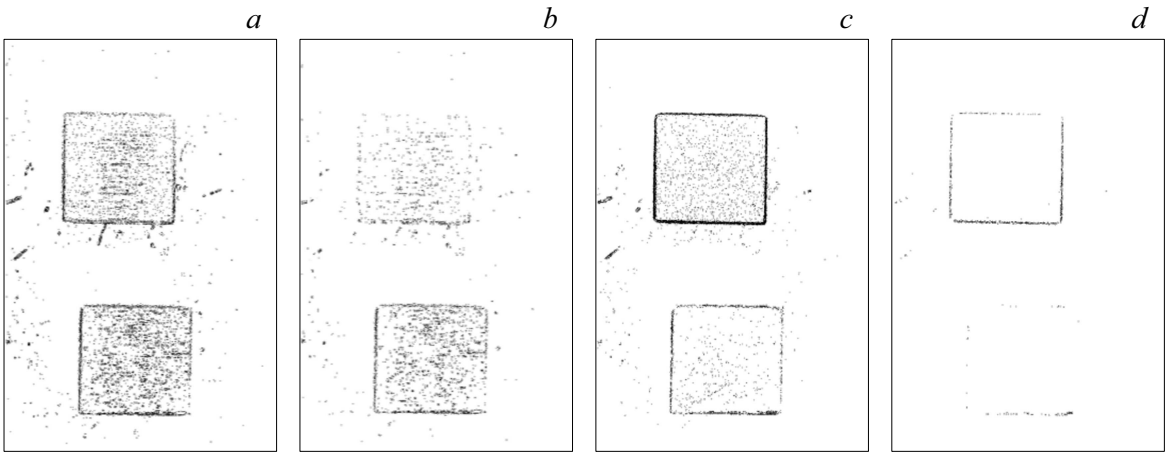

Figure 8. The result of spectral selection of HSI contours at $P_{f0} = 10^{-3}$, acceptance of hypotheses H_1, H_2, and different set of parameters $\Theta_{2,3,4}$: *a* — $\Theta_2 = 9$, $\Theta_3 = 1$, $\Theta_4 = 15$ for HSI set of Fig. 2, *b* — $\Theta_2 = 15$, $\Theta_3 = 10$, $\Theta_4 = 5$ for the same HSI set, *c* — $\Theta_2 = 9$, $\Theta_3 = 1$, $\Theta_4 = 15$ for HSI set of Fig. 3, *d* — $\Theta_2 = 15$, $\Theta_3 = 1$, $\Theta_4 = 15$ for the same HSI set.

operator masks [3]. Fig. 6 shows averaged values of gradients of several points of contour, where curve *1* — object 1 and background, *2* — object 1 and shadow, *3* — object 2 and background, *4* — object 2 and shadow. Fig. 7 shows structural functions corresponding to them, by changes of which the spectral selection of a specified object will be done, according to expressions (18)–(23). As an example, Fig. 8 shows options of spectral selection of the contours of objects at different values of the parameters $\Theta_{2,3,4}$ both for images distributed over the spectrum, and within a narrow spectral region.

Analysis of Figs. 6–8 have shown that the use of several spectral images within certain ranges allows to more clearly distinguish the regions of the gradient values and structural functions corresponding to them. According to [20], selection of the most informative spectral components allows to decrease the losses in confidence during recognition by limited number of spectral channels. This is why the selection of the most informative spectral components can be made at the imaging planning stage based on the information a priori about the observed objects and background or during the imaging with the controlled fragmental registration by spectrum, for example, based on acoustic and optic filters [2,21].

Quick action of the developed algorithm of the MathCad software tool, when processing the HSI with the size of 600×900 pixels by six most informative spectral components on a PC with the Intel Celeron CPU G1610 2.6 GHz processor and RAM of 2 GB was 40 s, out of which 36 s — only the first stage. Reduction of the processing time at the first stage is possible through optimizing the software code.

Conclusion

Therefore, the developed method in optimum setup allows to perform the spectral selection of the specified objects by their contours. It was found that several most informative HSI components obtained within certain spectral ranges are enough for the method?s efficient operation.

The developed method is implemented in the software and can be used in various hyperspectral systems, where spectral selection of the specified objects is required, for example, in medicinal hyperspectral modules for diagnostics of abnormal formations, in the non-destructive testing or in the operative environment monitoring systems.

Acknowledgments

The authors thank the acoustic and optical spectrometry laboratory of the Research and Engineering Center of the Unique Devices of the Russian Academy of Sciences for the assistance in performance of hyperspectral imaging of the objects.

Conflict of interest

The authors declare that they have no conflict of interest.

References

[1] A.N. Vinogradov, V.V. Egorov, A.P. Kalinin, A.I. Rodionov, I.D. Rodionov. Opticheskiy Zhurnal, **88** (4), 54 (2016) (in Russian)
[2] V.E. Pozhar, A.S. Machikhin, M.I. Gaponov, S.V. Shirokov, M.M. Mazur, A.E. Sheryshev. Light & Engineering, **27** (3), 99 (2019). DOI: 10.33383/2018-029.
[3] R. Gonzalez, R. Woods. *Tsifrovaya obrabotka izobrazheniy.* 3rd edition. (Tekhnosfera, Moskva, 2019) (in Russian)
[4] A.I. Perov, G.G. Sokolov. Radiotekhnika, **7**, 83 (1998) (in Russian)
[5] A.A. Sirota, A.I. Solomatin. Komp'yuternaya optika, **34** (1), 109 (2010) (in Russian)
[6] A.A. Sirota, A.I. Solomatin. Vestnik VGU, seriya: sistemniy analiz i informatsionnye tehnologii, **1**, 58 (2008) (in Russian)
[7] C.P. Huang, R.Z. Wang. Pattern Recognition and Image Analysis, **16** (3), 406 (2006).
[8] K.D. Grebenshikov, A.A. Spektor. Avtometriya, **4**, 119 (2001) (in Russian)
[9] P.A. Chochia. Informatsionnye protsessy, **14** (2), 117 (2014) (in Russian)
[10] R.A. Shovengerdt. *Distantsionnoe zondirovanie. Modeli i metody obrabotki izobrazheniy* Tekhnosfera, Moskva, 2013) (in Russian)
[11] T.A. Sheremetieva, G.N. Filippov, A.M. Malov. J. Opt. Tech., **82** (1), 24 (2015).
[12] V.V. Shipko, E.A. Samoilin, V.E. Pozhar, A.S. Machikhin. Optoelectronics, Instrumentation and Data Processing, **57** (6), 618 (2021). DOI: 10.3103/S8756699021060145.
[13] V.V. Shipko. Tsifrovaya obrabotka signalov, **4**, 36 (2021).
[14] *Sovremennye tekhnologii obrabotki dannykh distantsionnogo zondirovaniya Zemli,* edited by V.V. Eremeeva (Fizmatlit, Moskva, 2015) (in Russian)
[15] V.G. Repin, G.P. Tartakovskiy. *Statisticheskiy sintez pri apriornoy neopredelennosti i adaptatsiya informatsionnykh sistem* (Sovetskoe radio, Moskva, 1977) (in Russian)
[16] B.R. Levin. *Teoreticheskie osnovy radiotekhniki.* Book 2. (Sovetskoe radio, Moskva, 1968) (in Russian)
[17] M.F. Volobuev, V.A. Ufaev. Informatsionno-izmeritelnye i upravlyaushchie sistemy, **15** (10), 28 (2017) (in Russian)
[18] E.S. Ventsel, L.A. Ovcharova. *Prikladnye zadachi teorii veroyatnostei* (Radio i svyaz, Moskva, 1983) (in Russian)
[19] I.N. Bronshtein, K.A. Semendyaev. *Spravochnik po matematike dlya inzhenerov i uchashchikhsya VTUZov* (Nauka, Moskva, 1980) (in Russian)
[20] I.A. Kozinov, G.N. Maltsev. Opt. Spectrosc., **121** (6), 934 (2016).
DOI: 10.1134/S0030400X16120158.
[21] M.M. Mazur, Y.A. Suddenok, V.E. Pozhar. Opt. Spectrosc., **128** (2) 274 (2020). DOI: 10.1134/S0030400X20020162.